



# Projected changes in the mean and intra-seasonal variability of the Indian summer monsoon in the RegCM CORDEX-CORE simulations under higher warming conditions

Namendra Kumar Shahi<sup>1,5</sup> · Sushant Das<sup>2</sup> · Soumik Ghosh<sup>3</sup> · Pyarimohan Maharana<sup>4</sup> · Shailendra Rai<sup>5</sup>

Received: 25 December 2020 / Accepted: 12 April 2021 / Published online: 21 April 2021

© The Author(s), under exclusive licence to Springer-Verlag GmbH Germany, part of Springer Nature 2021

## Abstract

The present study employed the latest high-resolution regional climate model (RegCM4), driven by MPI-ESM-MR boundary conditions from the CORDEX-CORE South Asia framework to investigate the possible projected changes in the mean and intra-seasonal variability of the Indian summer monsoon (ISM) precipitation and their associated dynamics during near future (NF; 2041–2060) and far future (FF; 2080–2099) with respect to the historical period (1995–2014) under RCP8.5 scenario. Extensive evaluation analysis indicates that the RegCM4 is fairly able to simulate the spatial-temporal distribution of the observed mean and extreme precipitation, low-level jet, and intra-seasonal variability i.e. active and break composite patterns of the precipitation anomalies over India during the historical period. A substantial decline in the projected precipitation during ISM is estimated over central and northwest India in NF (about 10–30%) as well as in FF (upto 50%), which may be attributed to the weakening and northward shift of low-level winds. The occurrences as well as the intensity of the extreme precipitation events are expected to increase over India in the future. The precipitation during the projected active spells will escalate over the monsoon core region. This is supported by the decrease in sea level pressure over land, which favors the winds to transport more moisture from the adjoining seas for the formation of convective clouds, which is partly indicated through the decline in net surface longwave radiation. On the other hand, the precipitation intensity during the projected break spells is expected to further decrease in the future.

**Keywords** Indian summer monsoon · Intra-seasonal variability of monsoon · RegCM4 · Future projection · MPI–ESM–MR

## 1 Introduction

Changing climate and its associated impacts have been an important issue of this century which scientists are in a continuous process to improve their level of understanding

(IPCC 2007; Pachauri et al. 2014). Several studies have provided evidence that at present the earth has warmed to about 1 °C relative to the pre-industrial era (Victor and Kenney 2014; Allen et al. 2018; Tollefson 2020). As there is a transition in the atmospheric constituents (e.g. increasing GHGs) due to rapid industrialization, use of fossil fuels, land use and land cover changes etc., a simultaneous change is observed in air temperature. This change in temperature is the manifestation of the disruption in the global energy balance, which ultimately influences other meteorological parameters e.g. precipitation, snow cover, wind circulations etc.. In general, the earlier studies employed various global climate models (GCMs) to investigate the responses of these climate variables to increasing GHGs concentrations (Mehraug et al. 2017; Xu et al. 2018; Rogelj et al. 2019). They mainly focused on providing a global picture of climate change signals in the analyzed variables. The GCM generated data could also be used to study the regional changes; however, these may not be that efficient in representing the

Namendra Kumar Shahi  
nkshahi2010@gmail.com;  
namendra-kumar.shahi@lmd.polytechnique.fr

<sup>1</sup> CNRS-IPSL Laboratoire de Météorologie Dynamique (LMD), École Polytechnique, 91128 Palaiseau, France

<sup>2</sup> Earth System Physics Section, The Abdus Salam International Centre for Theoretical Physics, Trieste, Italy

<sup>3</sup> Department of Geophysics, Institute of Science, Banaras Hindu University, Varanasi, India

<sup>4</sup> Faculty of Science, Sri Sri University, Cuttack, India

<sup>5</sup> K. Banerjee Centre of Atmospheric and Ocean Studies, University of Allahabad, Prayagraj, India

local responses. The reasons being a replication of regional phenomena e.g. local convections, topographical forcings, land use type, circulations etc. that GCMs may not be suitable to parameterize mostly due to their coarser resolutions (Stone and Risbey 1990; Bader et al. 2008; Kang et al. 2015). In order to resolve this issue associated with the GCM, the concept of dynamically downscaling technique through regional climate models (RCMs) was put forth (e.g. Giorgi and Bates 1989). The RCMs have significantly improved during the last 30 years (Giorgi 2019) and have been instrumental in providing climatic information over regional to local scale at a very finer resolution. The added value of RCMs over GCMs is well demonstrated by several studies especially over the complex topographical regions as well as tropical studies (Feser et al. 2011; Torma et al. 2015; Ciarlo et al. 2020). Regarding the dynamics too, the RCMs are well equipped in simulating through their physics provided it is well tuned over the region of interest (Giorgi et al. 2012). For region-specific studies, dedicated World Climate Research Programme (WCRP) projects like Coordinated Regional Climate Downscaling Experiment (CORDEX) were initiated (Giorgi et al. 2009). The project aims to provide high-resolution regional climate information across several CORDEX domains across the globe (Giorgi et al. 2012) at 50 km horizontal resolution. Later, further increasing the resolution (~25 km), a CORDEX-Coordinated Output for Regional Evaluations (CORE) project was initiated over all the CORDEX domains (Giorgi and Gutowski 2015). One of such domains is the South Asia CORDEX domain, which involves very complex topography and regional-driven processes that defines the weather and climate. One of the key features of this region, which is more dominant than any other region of the world, is the Indian summer monsoon (ISM). Several studies have discussed the possible future changes in the Indian summer monsoon under anthropogenic greenhouse warming scenarios (Rupa Kumar et al. 2006; Mandke et al. 2007; Dash et al. 2015; Sharmila et al. 2015; Ali et al. 2019; Mukherjee et al. 2018; Maharana et al. 2020a, 2020b). Nevertheless, the future projections of regional monsoons still remain largely uncertain in terms of rainfall estimates and need more careful investigations (IPCC, 2007; Pachauri et al. 2014).

ISM precipitation is a very crucial phenomenon, which by in large influences the agricultural-driven economy of most of the South Asian nations. The ISM precipitation is also highly variable in terms of its temporal and spatial variability, which makes it more complex and interesting (Shahi et al. 2016, 2018a). In general, the ISM onset occurs at 1st week of June at the Kerala coast, propagates northward till it reaches northwest India to Pakistan by 1st week of July and then withdrawal occurs till September end and therefore also referred to as JJAS (June to September) precipitation (Shahi et al. 2018b). Within this period, India receives about 80%

of annual precipitation (Maharana and Dimri 2014). The prediction and future projection of ISM precipitation have been quite a challenging task for the researchers due to several underlying physical processes involved. These processes vary from large-scale global phenomena like El-Nino Southern Oscillations (ENSO) to regional scale e.g. land use, topography, aerosols etc. Several RCM studies have shown their influence on ISM precipitation characteristics. Local to regional feedbacks in the form of flux exchanges between the land and atmosphere, urbanization have shown strong modulators of the ISM (Paul et al. 2016; Shastri and Ghosh 2018; Maharana et al. 2019a). Aerosols have been shown to modulate the ISM by modifying the thermal structure of the atmosphere and regional circulations (Maharana et al. 2019b; Das et al. 2020a). In particular, mineral dust aerosols could strengthen the ISM precipitation by facilitating more moisture from the Arabian Sea through dynamical feedback (Das et al. 2015). Das et al. (2020b) using RCM showed that aerosol deposition on the Himalayan and Tibetan Plateau snowpacks could generate simultaneous feedback processes that can affect ISM precipitation distribution.

The study of intra-seasonal variability using RCMs is one of the major areas of interest by many scientists (Bhaskaran et al. 1998; Taraphdar et al. 2010; Maharana and Dimri 2016; Bhatla and Ghosh 2015; Bhatla et al. 2016; Ghosh et al. 2019; Chen et al. 2018). A sensitivity study by Umakanth et al. (2016) demonstrated that regional climate model simulations (e.g. RegCM) are sensitive to the choice of convection scheme and initial and boundary condition (ICBC) (Ghosh et al. 2019). A number of precautions in the context of choosing the ICBC are very important for a reliable simulation of seasonal and intra-seasonal monsoon variability using RegCM4 (Ghosh et al. 2019). Other important physics options such as; convection schemes, planetary boundary layers, etc. are also sensitive to RegCM model simulations. For example, it has been found that the Emanuel convection scheme performed better in simulating the spatial characteristics of strong (dominated by high-frequency oscillations) and weak (dominated with low-frequency oscillations) monsoon years of the Indian summer monsoon (Umakanth et al. 2016). Maharana and Dimri (2016) have shown that the RegCM4 model is able to represent the precipitation, surface temperature, sea level pressure, lower level wind during the ISM season and different phases (active and break) of monsoon; also a negative and positive anomaly of outgoing longwave radiation (OLR) is identified during the active and break phases respectively (Bhatla et al. 2018). A high-resolution model output could be a better solution to avoid these uncertainties during the intra-seasonal time scale along with during other climatic conditions e.g. El Niño and La Niña (Maurya et al. 2020).

Considering the usage of RCM in the above literature, we attempt to investigate the change in ISM precipitation

using the RegCM4 regional climate model simulations driven by MPI-ESM-MR under the RCP8.5 scenario of the CORDEX-CORE South Asia domain simulation. For the control period, ERA-Interim driven RegCM4 simulations are also used. A recent study by Maharana et al. (2020a) inter-compared the different RCMs within the CORDEX-CORE project in the simulation of rainfall characteristics during ISM and found that most of the RCMs, while using MPI-ESM GCMs boundary conditions performed better than other driving GCMs. Therefore, in this paper, we chose the RegCM4 simulations driven by MPI-ESM-MR and carried out extensive analyses by taking several metrics i.e. spatial distribution of the mean, extremes, active and break composites, probability distribution functions. Further, the associated dynamics are also investigated. In the next section, details of the RegCM4 model and methodology are given.

## 2 Model, data, and methodology

We used the latest CORDEX-CORE simulated datasets from the RegCM4 model. To be precise, RegCM4 is a limited area sigma-coordinate model and is maintained and developed at the Abdus Salam International Centre for Theoretical Physics (ICTP). This model has been used widely to downscale climate information at the regional to local scale over multiple CORDEX domains (Giorgi et al. 2012). Previously, RegCM4 has been used for downscaling precipitation and temperature characteristics over the South Asia (Dash et al. 2006, 2009, 2015; Pattnayak et al. 2015; Maharana et al. 2019a). The model incorporates several physics parameterizations to represent the physical processes.

For the South Asia CORDEX domain, the convection is represented by MIT (Emanuel and Rothman 1999) over land and Tiedtke (1989) over the ocean. The land surface processes are implemented by coupling RegCM4 with the community land surface model version 4.5 (CLM4.5; Oleyson et al. 2013). The boundary layer evolution and radiation transfer scheme are represented by Grenier and Bretherton (2001) and Kiehl et al. (1996); respectively. The Subgrid Explicit Moisture Scheme (SUBEX) scheme is used for large-scale cloud formations (Pal et al. 2000). The domain consists of  $429 \times 337$  grids with 23 vertical levels. In the present work, we used ERA-Interim ( $\sim 0.75^\circ \times 0.75^\circ$ ) and MPI-ESM-MR ( $\sim 1.8^\circ \times 1.8^\circ$ ) driven RegCM4 simulations for our analysis, and the RegCM4 simulations are forced by the 6-hourly initial and lateral boundary conditions. Recently, the data were generated following the CORDEX-CORE protocol and are dynamically downscaled at 25 km. We chose three 20-year time slices i.e. 1995–2014 (historical period, HIST), 2051–2060 (near future period, NF), and 2080–2099 (far future period, FF) for carrying out the analysis. All the

analysis carried out is for the ISM i.e. JJAS period. The India Meteorological Department (IMD) gridded daily mean rainfall ( $0.25^\circ \times 0.25^\circ$ ) has been used as a reference dataset for the validation of the simulated precipitation. It is obtained from daily rainfall records from 6955 rain-gauge stations, which is till now the highest number of stations used for any kind of gridded data available over India (Pai et al. 2014). For the winds, the latest released ERA5 reanalysis dataset is utilized at a  $\sim 30$  km resolution grid (Hersbach et al. 2020).

A 10–90 day bandpass Lanczos filter (Duchon 1979) is used and applied on the daily total precipitation anomalies to extract the intra-seasonal variability of ISM precipitation from total precipitation (Goswami et al. 2006; Sharmila et al. 2015). A band-pass filter works by passing frequencies between the lower limit and the higher limit band (10–90 days in our case) and suppresses all variability outside the frequency range. The actual calculation consists of two steps. In the first step, it transforms each grid point of the dataset into a frequency domain. Then certain frequencies are filtered in the frequency domain and the spectrum is transformed back into the time domain. The numerical procedures of the bandpass method are described in more detail in the Duchon (1979). As we know that in order to simulate a realistic summer mean monsoon, a model needs to properly simulate the internal variability, and most of this internal variability is generated by the low-frequency intraseasonal oscillations (ISOs). It has been demonstrated that ISOs have a broadband power spectrum with periodicities between 10 and 90 days or in other words, we can say that the variability due to the ISOs lies within the period range of 10–90 days, which allows the probability of occurrence of positive and negative phases to be different and could contribute to the seasonal mean (Goswami and Xavier 2005; Goswami 2012; Waliser 2006; Wang 2012). Therefore, to relate the intraseasonal anomalies to the seasonal mean monsoon, a 10–90 day bandpass Lanczos filter is used in the present study to extract the total monsoon intraseasonal anomalies. To identify the active and break spells associated with the summer monsoon intra-seasonal variability, a monsoon index is computed as the area-averaged precipitation anomalies over the monsoon core region (MCR; Rajeevan et al. 2010) for each JJAS season normalized by its own standard deviation. The MCR region/box is shown in Fig. 2a. The active (break) periods are identified such that monsoon index  $>= +1.0$  ( $\leq -1.0$ ) for at least consecutive 2 days or more. The probability density function (PDF) is used in the study to showcase the overall distribution of a variable over a region (Torma et al. 2015), where the PDF tails represent the precipitation extremes with its probability of occurrence over time. In addition, the spatial distribution of the precipitation percentage due to 95th and 99th percentile events is also computed during ISM.

### 3 Results and discussion

#### 3.1 RegCM4 model evaluation

To begin with, we first evaluated the time-latitude variation (Hovmöller plot) of the 20-year climatological mean precipitation averaged over the longitude 70°–90°E as shown in Fig. 1. The Hovmöller plot represents the development, maturity, and demise of ISM precipitation in the RegCM4 simulations compared against IMD (Fig. 1). From Fig. 1, it is quite evident that the onset of ISM takes place around in the month of June and it propagates northward along the

Indian landmass and reaches the northern limit of the Indian subcontinent during July and August, and rapidly withdraws in September. A clear northward propagation of monsoon precipitation from June to August and then the southward movement from September to November can be clearly seen from the observation and the RegCM4 simulations captured it significantly (Fig. 1). However, the model slightly underestimates (~1 mm/day) the precipitation between the latitudinal bands (20°–26°N) during the summer and slightly overestimates the precipitation between the latitude 9°–19°N during the months of August to November (Fig. 1b–c). Further, the simulated precipitation above the latitude 31°N is relatively higher possibly due to the orographic effect. Other than this, the latitudinal variation of the ISM is well represented in both the simulations, but the intensity of the precipitation varies slightly among the RegCM4 simulations.

The spatial pattern of 20-year climatological June–September (JJAS) seasonal mean precipitation during the historical period over the Indian subcontinent for the IMD observation and the RegCM4 simulations along with their biases are shown in Fig. 2. The RegCM4 simulation, in both cases, quite effectively captures the spatial distribution of the observed precipitation pattern with spatial accuracy over India. On the other hand, both simulations have quite well simulated the observed maxima of precipitation over the Western Ghats, Northeast India, the foothills of the Himalayas, and the east central parts of the India (Fig. 2a–c). Apart from areas with heavy rainfall, the northwest regions with the least precipitation (~1–3 mm/day) are also well represented by both simulations. The bias map depicts that the RegCM4 shows wet bias over northeastern states and parts of peninsular India. The reasons could be due to enhanced topographical forcings and also partly attributed to the use of the CLM4.5 scheme in the model experiments as previously reported by Halder et al. (2015). We notice a significant improvement (less bias) in the JJAS mean precipitation over the central parts of India, which was strongly underestimated (larger bias) in previous CORDEX experiments (Singh et al., 2017; Choudhary et al., 2018; Rana et al., 2020), and the marked improvement in the representation of precipitation in the latest model experiments (CORDEX-CORE) can be attributed to the improvement in physics and resolution compared to the previous CORDEX experiments. Interestingly, the seasonal mean precipitation variation over the central India is better represented in RegCM4\_MPI than RegCM4\_EIN as noticed due to lesser dry bias. It is known that model simulations are dependent on many factors. Here, in our case, we have used a similar configuration i.e. same physics and resolutions except for the initial and lateral boundary conditions (IC-LBCs) information in both RegCM experiments, and therefore we can say that the quality of the IC-LBCs could be a possible reason for this result. Previous studies have also indicated that the simulation of Indian summer

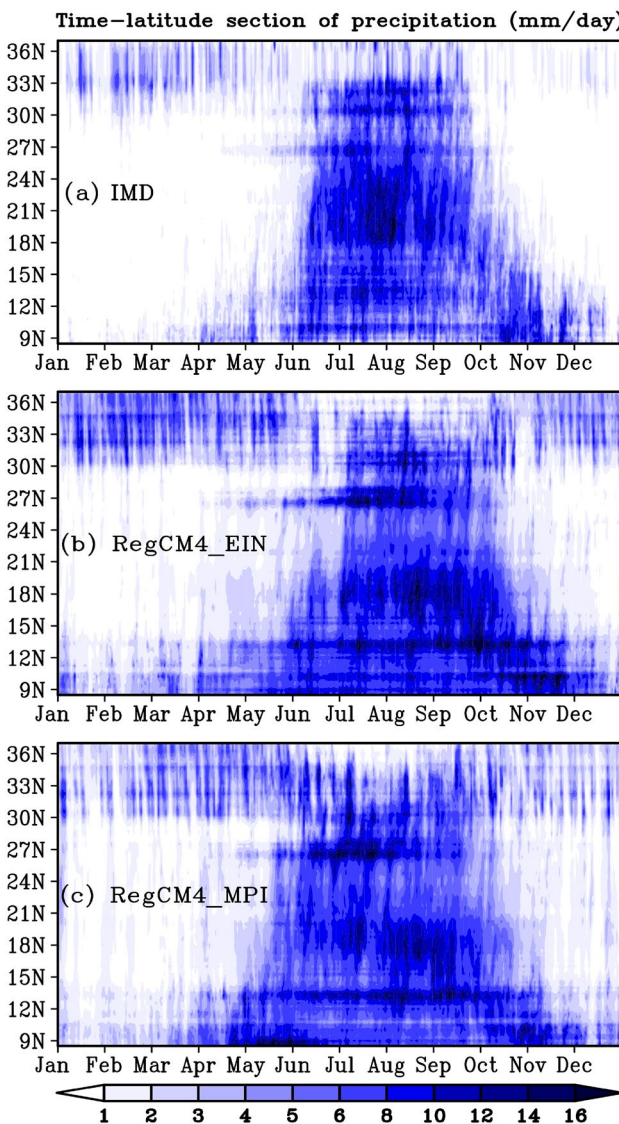


**Fig. 1** Time-latitude section of daily climatological mean precipitation averaged over the longitude 70°E–90°E for (a) IMD, (b) RegCM4\_EIN, & (c) RegCM4\_MPI during 1995–2014. Units are in  $\text{mm day}^{-1}$

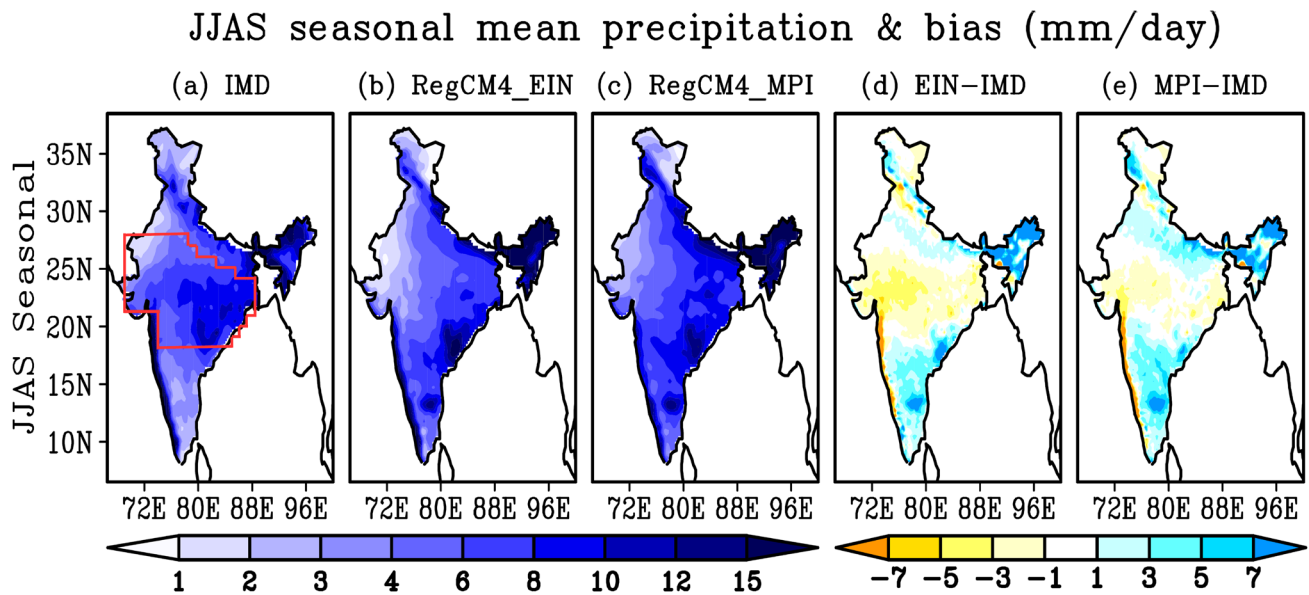


**Fig. 2** JJAS seasonal climatological mean precipitation for (a) IMD, (b) RegCM4\_EIN, & (c) RegCM4\_MPI and the corresponding bias for (d) RegCM4\_EIN minus IMD, and (e) RegCM4\_MPI minus IMD during 1995–2014. Units are in  $\text{mm day}^{-1}$

monsoon precipitation using the RegCM model is very sensitive to the choice of the IC-LBCs (Ghosh et al. 2019). We have also calculated the annual cycle of precipitation averaged over the Indian landmass and MCR for the evaluation (Fig. 3). Comparative analysis shows that RegCM4 captures the annual cycle of observed precipitation over both regions (Indian landmass and MCR) quite well. Over the Indian landmass (Fig. 3a), the RegCM4\_EIN and RegCM4\_MPI simulated precipitation are in agreement with the observed mean variability (i.e. low values in winter and high values in summer) despite some overestimation ( $\sim 1\text{--}2 \text{ mm/day}$ ).

While over the MCR (Fig. 3b), the RegCM4\_MPI simulated precipitation is almost similar to the IMD observation in the monsoon months of July, August, and September, and overestimates during the months of June. The RegCM4\_EIN slightly underestimates the precipitation in the months of June, and July, and overestimated the precipitation in the months of September. In the non-monsoon months, both simulations overestimate the precipitation ( $\sim 1\text{--}2 \text{ mm/day}$ ) over both regions.

For quantitative analysis, the annual and JJAS (in brackets) correlation coefficient (CC) of observation with

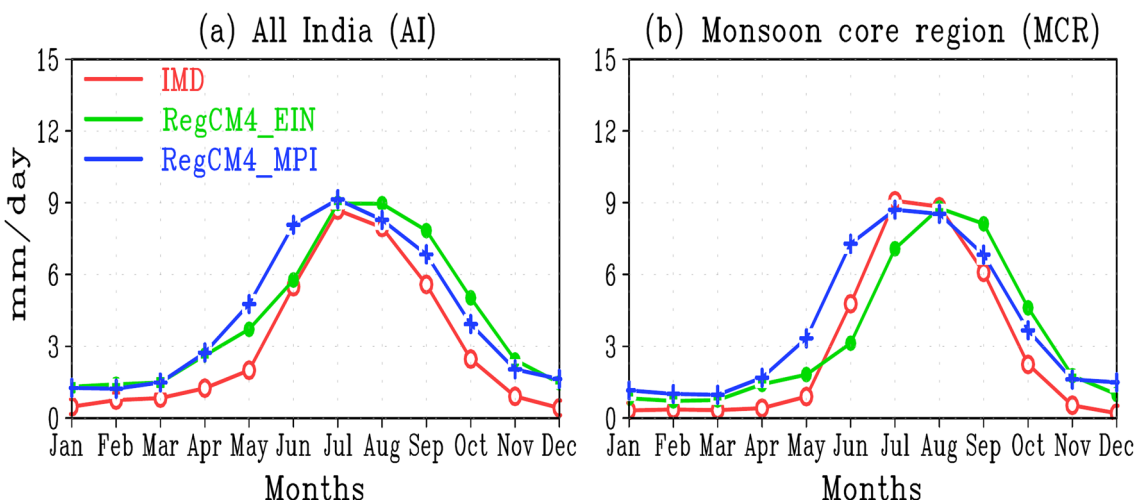


**Fig. 3** Annual cycle of area-averaged mean precipitation over (a) All India, and (b) Monsoon core region (MCR) from the IMD, RegCM4\_EIN, and RegCM4\_MPI during 1995–2014. Units are in  $\text{mm day}^{-1}$

RegCM4\_EIN and RegCM4\_MPI is 0.95 (0.77) and 0.94 (0.73) over the Indian landmass, and 0.91 (0.62) and 0.92 (0.67) over the MCR; respectively (Table 1). The value of the index of agreement (IOA; Shahi et al. 2019) is also high ( $> 0.9$ ) & ( $> 0.67$ ) for the annual & JJAS; respectively over both regions that are all India and MCR (Table 1). The strong CC and the low root mean square error (RMSE) values, and the closer standard deviation value with the observed one indicate good quality of the simulations. In addition, the results suggest that the performance of the

**Table 1** The annual and JJAS correlation coefficient ( $r$ ), index of agreement (IOA), and root mean square error (rmse) of IMD with RegCM4\_EIN and RegCM4\_MPI over the All India and Monsoon Core Region (MCR) are given

Statistics	All India (AI)		Monsoon core region (MCR)		
	Annual	JJAS	Annual	JJAS	
$r$	RegCM4_EIN	0.95	0.77	0.91	0.62
	RegCM4_MPI	0.94	0.73	0.92	0.67
IOA	RegCM4_EIN	0.94	0.79	0.93	0.73
	RegCM4_MPI	0.93	0.68	0.93	0.67
RMSE	RegCM4_EIN	1.50	1.50	1.65	2.25
	RegCM4_MPI	1.60	1.70	1.71	2.00
SD	IMD	3.01	1.83	3.46	2.44
	RegCM4_EIN	2.94	1.45	3.03	2.40
	RegCM4_MPI	3.01	1.16	3.10	1.31

The annual and JJAS standard deviation (SD) of IMD, EIN, and MPI over All India and MCR are also given

RegCM4\_MPI is relatively better than the RegCM4\_EIN over the MCR implying its reliance for the future projection as carried out in this study.

The JJAS seasonal mean wind (at 850 hPa) simulated by RegCM4\_EIN and RegCM4\_MPI are compared with the ERA5 reanalysis (Fig. 4). The 850 hPa wind is chosen for the analysis as maximum moisture gets transported toward the Indian landmass from the adjacent Oceans at this pressure level and therefore also known as the monsoon low-level jet (Dash et al. 2006). The strength of the low-level jet also determines its relative contribution to the precipitation extremes during the ISM (Roxy et al. 2017). Both the simulations have quite reasonably well captured the observed spatial features of the climatological low-level circulation pattern such as the Somalian Jet over the Arabian Sea, and cross-equatorial flow (Fig. 4a–c). Further, the estimated pattern correlation coefficient of monsoon low-level jet simulated in RegCM4\_EIN (RegCM4\_MPI) with that of ERA5 is 0.90 (0.86) indicates a good representation of the circulation pattern and an improvement in the associated dynamical features across the domain during ISM. The simulated wind speed is slightly overestimated in the region of the western parts of India (Fig. 4b–c), which may also be a possible reason for contributing dry bias over it (Fig. 2).

To evaluate the magnitude of the precipitation extremes, we computed the PDFs of the daily mean precipitation over all India and the MCR (Fig. 5). In the case of the low to moderate intensity precipitation events, both simulations are very close to the IMD observation. On the other hand, the RegCM4 simulations significantly overestimate the

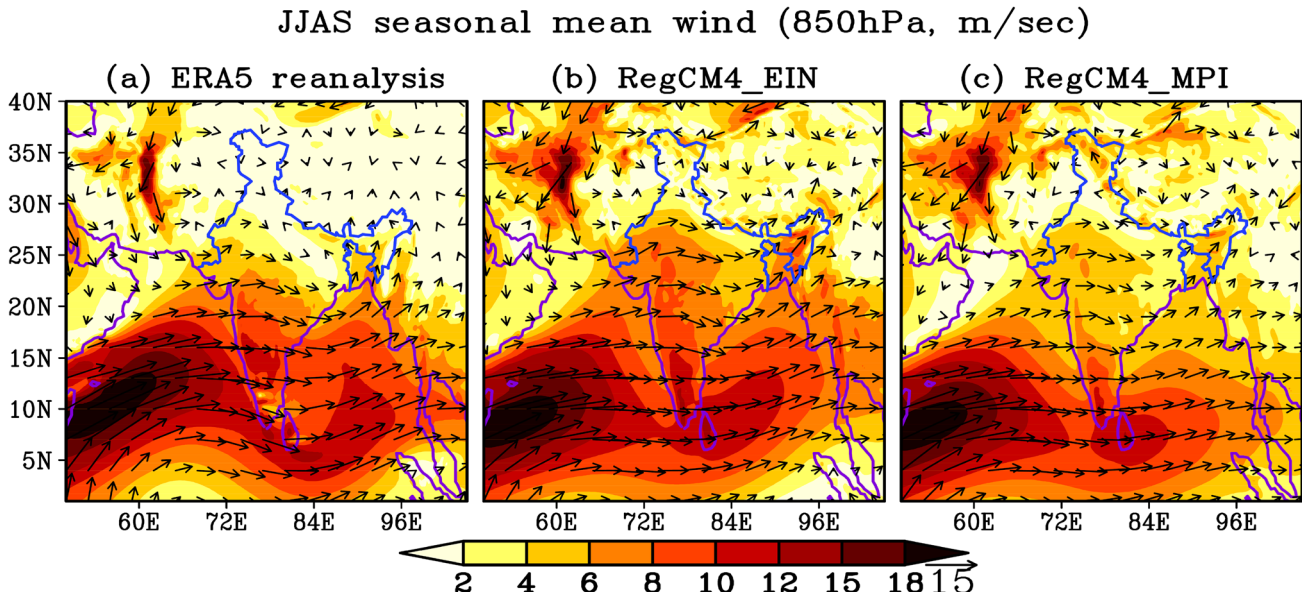


**Fig. 4** JJAS seasonal climatological mean wind for (a) ERA5 reanalysis, (b) RegCM4\_EIN, and (c) RegCM4\_MPI during 1995–2014. Units are in  $\text{m s}^{-1}$

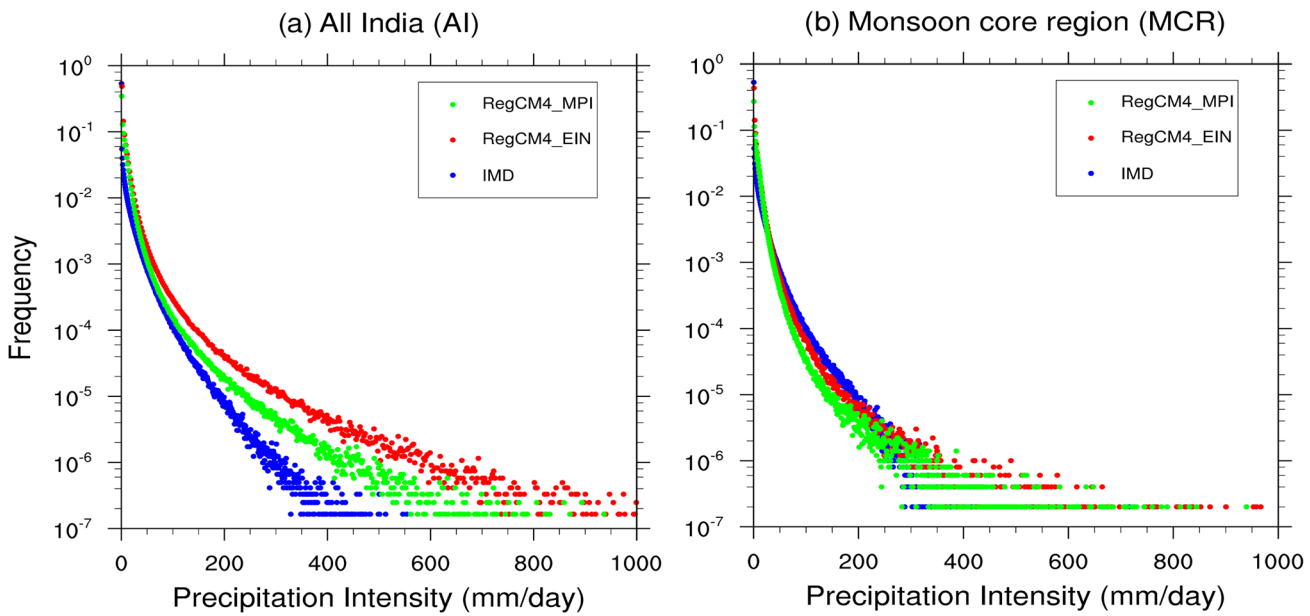


**Fig. 5** Probability density function (PDF) of daily mean precipitation over (a) All India, and (b) MCR during JJAS 1995–2014. Units are in  $\text{mm day}^{-1}$

occurrence of the high to very high-intensity precipitation events ( $> 200 \text{ mm/day}$ ) as indicated by the longer tails. Since all the grid points of the Indian landmass have been considered in this case, the regions with a complex topography (the western Himalayas, northeast hilly regions) contribute to such high-intensity events. In addition, the network of IMD rain gauge stations is very sparse over these regions thereby having considerable uncertainty in measurements as well, particularly for studying extreme events. We have also noted that the RegCM4\_MPI PDF curve is relatively closer to the observation than the RegCM4\_EIN (Fig. 5a). In the MCR (Fig. 5b), the observed intensity tail has been relatively well reproduced by both simulations. However, both simulations slightly underestimate the occurrence of observed moderate-intensity events and this difference may be due to the IMD observational uncertainties in the estimation of excessive rainfall. Although, the simulation and prediction of extreme events by numerical models is still a challenging task and climate scientists keep on employing various strategies to simulate it. The spatial variability of the precipitation extremes in terms of the percentage of precipitation contribution (P95) due to 95th percentile events is shown in Fig. 6. Here, the model well simulates the observed spatial distribution with high precipitation contributions in north, northwest, and southern India. Similar to the IMD observation, a more prominent pattern of P99 (percentage of precipitation due to 99th percentile events) is seen in northwest India (data not presented). As we know that the northwestern part of the India receives much less precipitation (as well as their number) than the rest parts of the country;

hence these precipitation days most of the time exceeds the P95/P99 in this region.

We further look into the active and break phases of summer monsoon intraseasonal variability of the ISM. For this, we have constructed the spatial composites pattern of active (break) spells using the 10–90 day filtered precipitation anomalies during 1995–2014 for IMD, RegCM4\_EIN, and RegCM4\_MPI (Fig. 7). The active (break) composite pattern obtained from the IMD shows the wet (dry) precipitation anomalies over the MCR including western India, Western Ghats, and dry (wet) precipitation anomalies over the south-eastern, northern parts of India, and Himalayan foothills regions. The IMD composite of the active spells reflects that the precipitation anomaly over the MCR is high by a magnitude of 6  $\text{mm/day}$  and more (Fig. 7a1). This can be attributed to the activity of the monsoon trough around the MCR (Maharana et al. 2016). The precipitation anomalies around the south-eastern, northern parts of India and the foothills of the Himalayas are negative, indicating relatively less or no precipitation during the active phase of the monsoon. The higher precipitation anomalies can be observed as the east–west stretch over the India subcontinent. The simulated precipitation distribution mimics the observed one with higher values over MCR and lower values over foothills and southern India. The precipitation band in the model simulations, however, shows a bit northward stretch instead of the westward stretch as observed in IMD. The RegCM4\_EIN (Fig. 7b1) has a more prominent northward stretch as compared to the RegCM4\_MPI (Fig. 7c1). In terms of dynamics, the RegCM4 simulations forced by EIN

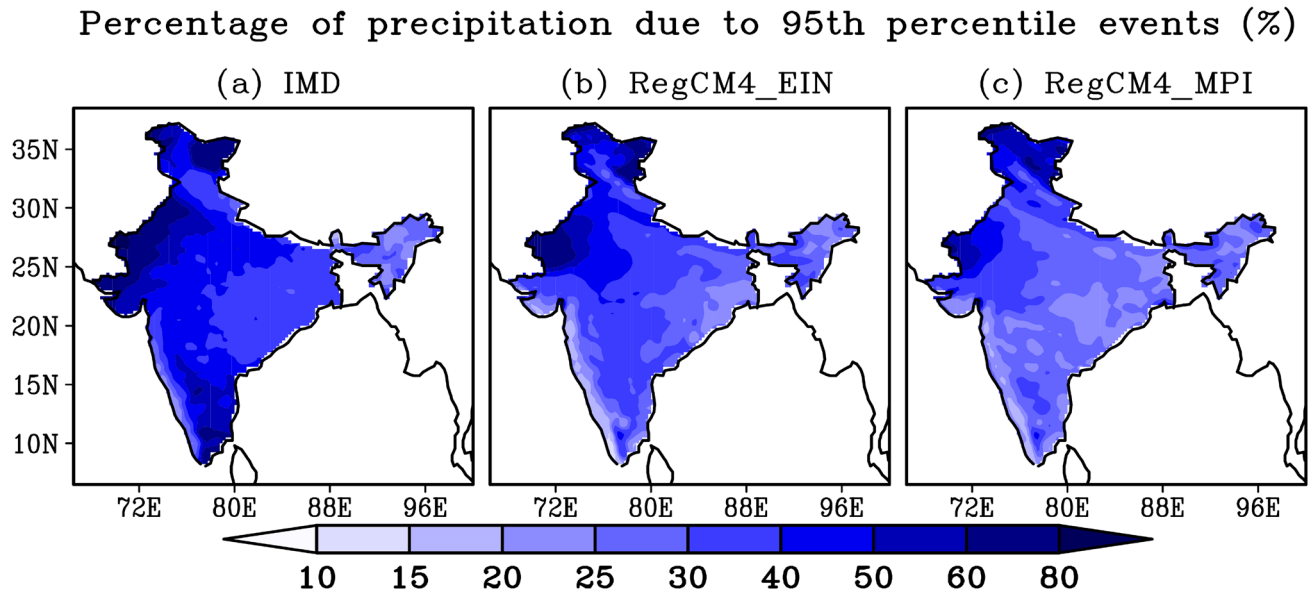


**Fig. 6** Percentage of precipitation (%) due to 95th percentile events for (a) IMD, (b) RegCM4\_EIN, and (c) RegCM4\_MPI during 1995–2014

and MPI show a significant decline in the pressure by 150 to 200 over the MCR in the historical period (Fig. 8a1–a2). This increases the pressure difference between land and sea leading to strong moisture incursion toward the MCR with the wind and hence increases the precipitation during active days (Fig. 8a5–a6). As a supportive analysis, negative anomalies of the net surface longwave radiation (NSLR, which is the difference between Surface Downwelling Longwave and Upwelling Longwave Radiation) over the Indian region also indicates that the more longwave radiation is emitted by the earth than it gains from the air, which can be attributed to the increased convective activities over the land (Fig. 8a3–a4). The wind pattern is the manifestation of the regional pressure pattern. Hence, the distributions of the sea level pressure (SLP) will play a major role in deciding the wind pattern during the active and break periods. Figures 8a5–a6 represent the composite wind patterns during the active days for both the RegCM4 simulations. The negative SLP anomaly over MCR brings in the wind from the ocean towards land. A relatively stronger wind over the MCR and Indo-Gangetic Plain (IGP) is found, which transports the moisture from the sea towards land and causes precipitation in MCR (Fig. 7b1–c1). Here, the topography i.e. the Himalayan foothills diverting the winds towards the west due to which we notice active cases in northwest regions.

During the break spells of the ISM, the MCR region experiences less or no precipitation. The observed composites of the break spells have a similar spatial structure with the active spells over India where the positive precipitation anomalies have been replaced by the negative precipitation anomalies by a magnitude below 6 mm/day (Fig. 7). While positive

precipitation anomalies or increase in precipitation over the foothills of the Himalayas, southeastern and northeast parts of India is detected during the break period (Figs. 7a2–c2) and it is well consistent with the negative NSLR anomalies indicating convective activities in these regions (Fig. 8b3–b4). Both RegCM4\_EIN and RegCM\_MPI correctly captured the spatial structure of the composite break days with a maximum decline of precipitation over MCR (Fig. 7b2–c2). Similar to the active days, the break composite also shows a northward stretch of the negative precipitation anomalies. Here, opposite patterns with respect to active phases are observed in the analysis of the dynamics i.e. increases in SLP (Fig. 8b1–b2) with the positive NSLR anomalies (Fig. 8b3–b4) over the MCR, and the winds are mostly northwesterly (Fig. 8b5–b6). Such conditions decline the moisture transport towards MCR, reduce convective processes, and therefore lead to the decrease in the precipitation over the MCR.

Overall, the extensive analysis revealed that the RegCM4 simulation driven by both EIN75 and MPI-ESM-MR boundary conditions is able to reasonably well capture the basic features of the ISM characteristics. Therefore, it gives us confidence in further investigating the projected changes in the ISM characteristics and its associated dynamics in the NF and FF driven by MPI-ESM-MR under the RCP85 scenario.

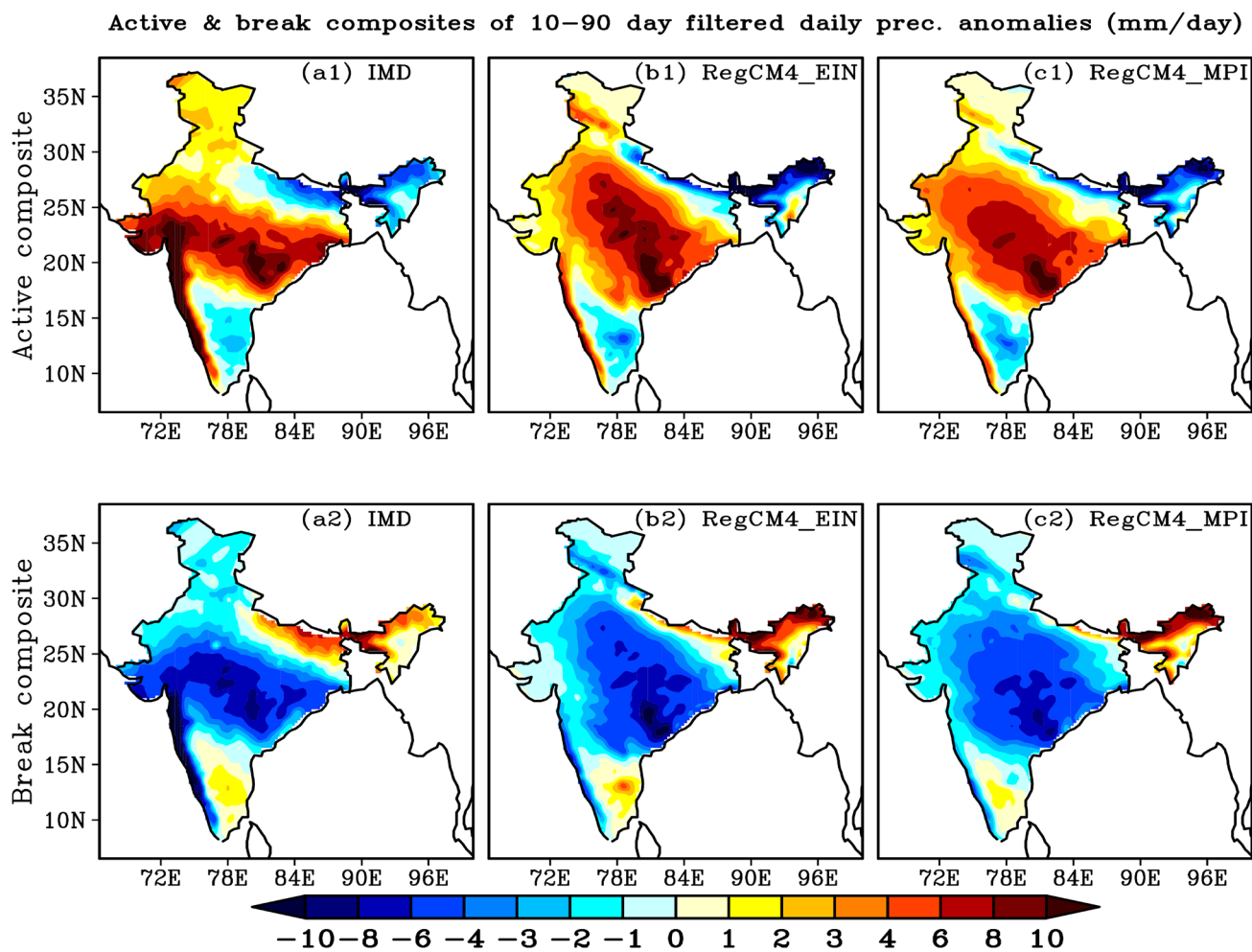


**Fig. 7** Active composite of 10–90 day filters daily precipitation anomalies for **(a1)** IMD, **(b1)** RegCM4\_EIN, and **(c1)** RegCM4\_MPI during 1995–2014. Similarly, the break compositions for IMD,

RegCM4\_EIN, and RegCM4\_MPI are shown in **a2**, **b2**, and **c2**; respectively. Units are in  $\text{mm day}^{-1}$

### 3.2 Future changes in the mean and intra-seasonal variability of summer monsoon and associated dynamics

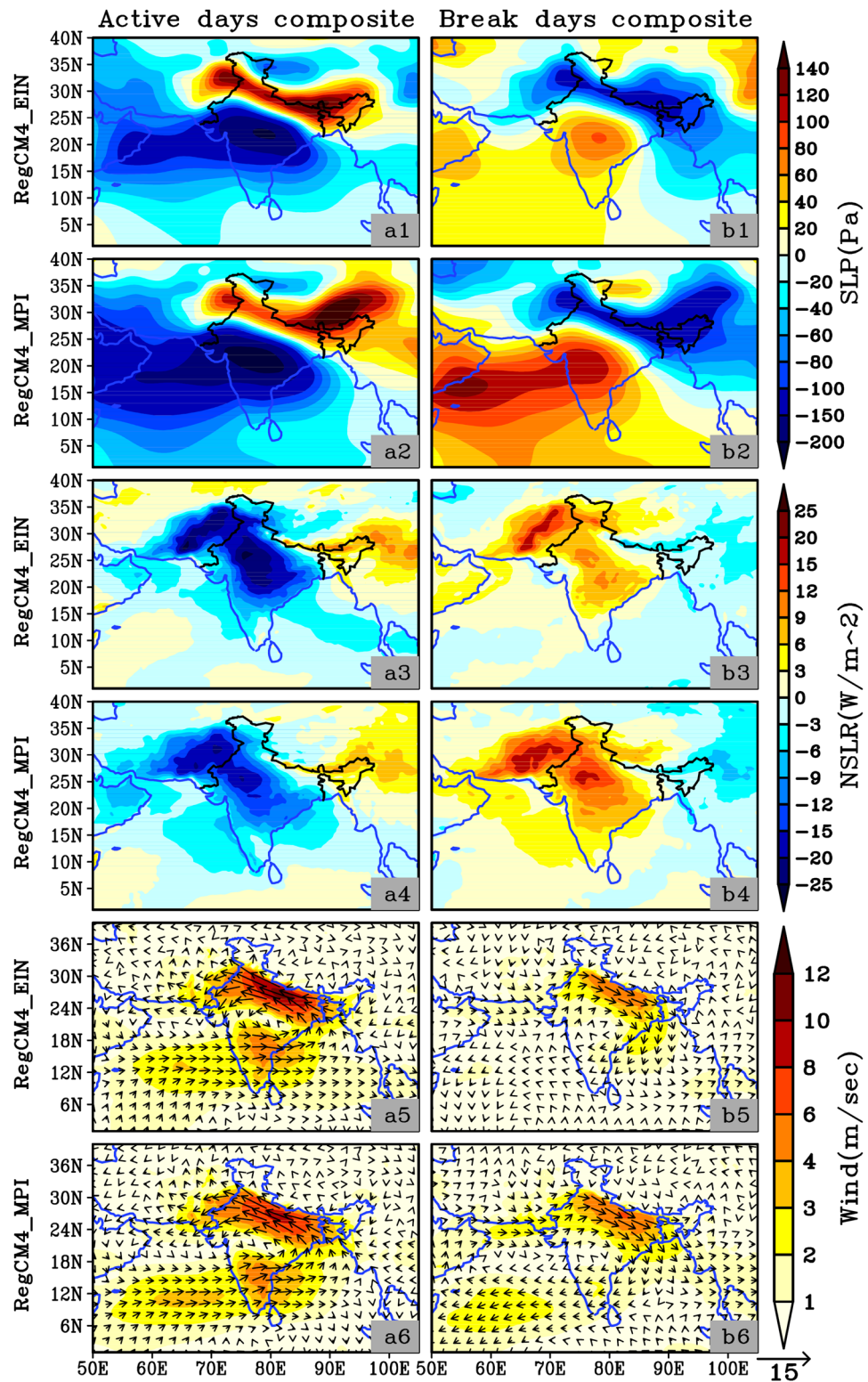
#### 3.2.1 Seasonal mean and extreme of summer monsoon precipitation

The RegCM4\_MPI simulated JJAS seasonal mean precipitation over India under the RCP8.5 scenarios for the NF, FF, and the projected relative changes with respect to the historical period (1995–2014) are shown (Fig. 9). RegCM4\_MPI projections indicate that the summer mean precipitation will decrease about 10–30% in the NF to about 20–50% in the FF over most parts of India except some parts of the northeast India and western Himalayan region, where the projections indicate the increase of the same by 10–30% and 40–60% in the NF and FF; respectively (Fig. 9c–e) relative to the present climate. The maximum decrease in the mean

precipitation (more than 40%) is found over northwest India in both NF and FF.

From a dynamic point of view, the JJAS seasonal wind pattern for NF and FF and their projected relative changes with respect to the historical period are presented (Fig. 10). The analysis shows a consistent decline in the wind strength especially over the Arabian Sea (between  $0^\circ$  and  $15^\circ\text{N}$ ) where the maximum strength of the wind is generally observed in both NF and FF (Fig. 10c–d). The decline in the wind strength leads to a decrease in moisture transport towards the Indian landmass from the Arabian Sea leading to the projected decreases in precipitation as discussed earlier and it is consistent with the finding of Dash et al. (2015). Apart from the weakening of the winds, there is also a northward shift in the winds with the more prominent signature in the FF. Previously, the northward shift of the winds was also found using GCM and RCM simulations (Sandep et al. 2014; Maharana et al. 2020b;

**Fig. 8** Active & break composites of (a1, b1, a2, b2) mean sea level pressure, (a3, b3, a4, b4) net surface longwave radiation, and (a5, b5, a6, b6) wind anomalies for RegCM4\_EIN and RegCM4\_MPI; respectively



Torres-Alavez et al. 2021). As the wind shifts northward, there is an enhancement of westerly winds coming from middle-west regions with less moisture content, which effectively reduces the moisture supply towards the Indian

landmass. These winds are warm and dry, which further inhibits the convection over India and in particular over the northwest regions where the highest decrease in precipitation is noticed in FF.

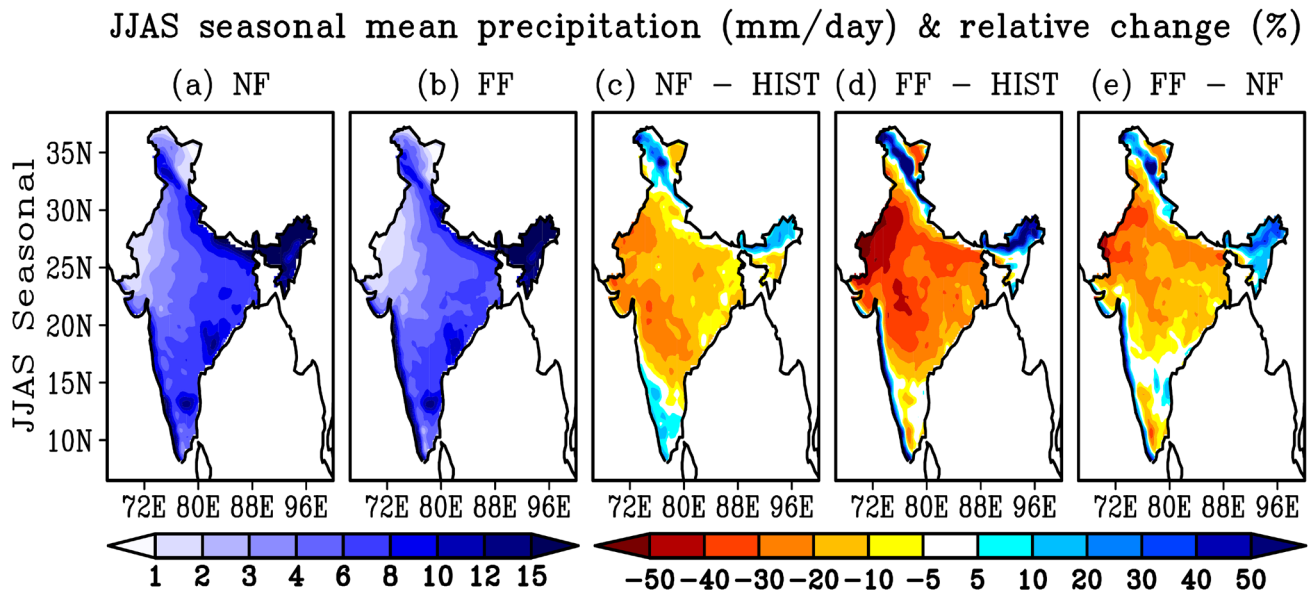


**Fig. 9** RegCM4\_MPI simulated JJAS seasonal climatological mean precipitation ( $\text{mm day}^{-1}$ ) during (a) NF, & (b) FF periods and the projected future relative changes (%) in the climatological mean precipitation in (c) NF minus HIST, (d) FF minus HIST, and (e) FF minus NF

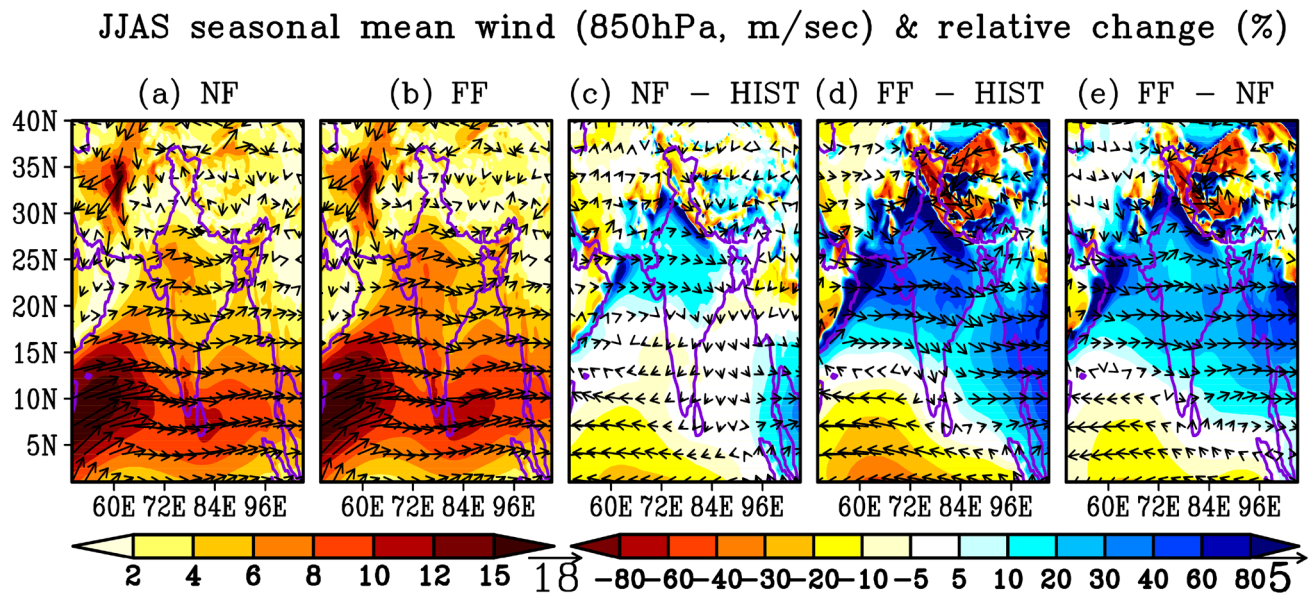


**Fig. 10** RegCM4\_MPI simulated JJAS seasonal climatological mean wind ( $\text{m sec}^{-1}$ ) during (a) NF, & (b) FF periods and the projected future relative changes (%) in the climatological mean wind in (c) NF minus HIST, (d) FF minus HIST, and (e) FF minus NF

The projected annual cycle of precipitation over all India and MCR with respect to the historical period is also examined (Fig. 11). A slight decline in the precipitation is noticed during the months of May–June in NF and FF when all India is considered (Fig. 11a, c). In the MCR region, the maximum decrease in the precipitation during the months of May–July (about 40%) is more pronounced in the FF period (Fig. 11b, d). One of the interesting points to mention is that the projected increase in

precipitation during the post-monsoon seasons (October to November) over both India and MCR. The increase in the precipitation particularly during the later months indicates a possible shift of the monsoon regime in the NF and FF periods under higher warming conditions over the MCR. It is in line with the results of Ashfaq et al. (2020), which indicated a possible shift in the monsoon onset and demise dates over the South Asian region under the RCP8.5 scenario.

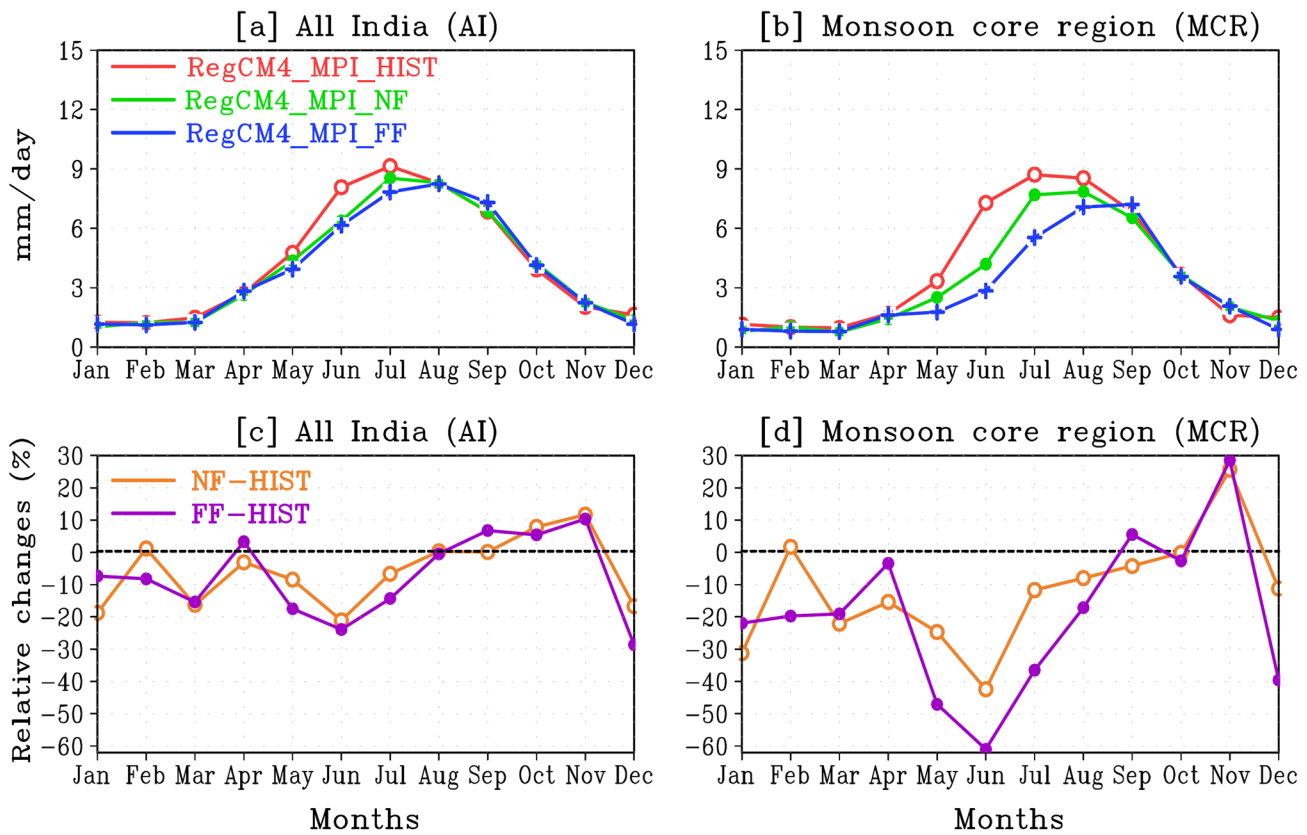


**Fig. 11** Annual cycle of mean precipitation ( $\text{mm day}^{-1}$ ) for (a) All India and (b) MCR during historical, near- and far-future periods. Bottom panel shows future changes (%) in the averaged mean precipitation over (c) All India, and (d) MCR as simulated by RegCM4\_MPI

We have computed the PDF of the daily mean precipitation over all Indian and MCR grid points for the NF, FF and plotted with the historical period to estimate future changes in extreme precipitation intensities (Fig. 12). A substantial increase in the occurrence of the medium to high-intensity events is observed in the NF and FF periods over the Indian landmass (Fig. 12a) and this indicates an increase in extreme precipitation events over entire India. Over the MCR, there is a slight increase in the occurrence of high-intensity events in the NF as well as FF periods (Fig. 12b). The earlier studies also have stated that the extreme events are expected to increase over India in the future climate scenarios (Pachauri et al. 2014; Mukherjee et al. 2018; Ali et al. 2019) and the findings of the present study are consistent with it. For spatially visualizing the precipitation extremes over India, we also plotted the precipitation percent due to R95 for both the future periods considered in the study (Fig. 13). In the NF, there is a sign of a small increase in the percentage contribution of extreme precipitation by 5–10% over the northwestern India (Fig. 13c), which gradually intensifies up to 20% with higher spatial coverage in the FF (Fig. 13d). However, the same trends decrease over some parts of western Himalayas by about 5–10% and 20% in the NF and FF; respectively.

### 3.2.2 Intra-seasonal variability of the ISM precipitation

Figure 14 represents the projected change in the behavior of the composite of the active and break spells in NF and FF with respect to the historical period. To be precise, the active periods gradually become more intense over MCR from NF to FF (Fig. 14a1–b1). In the NF, an increase of precipitation along the Indo Gangetic Plains (IGP) and northern MCR ( $\sim 1\text{--}3 \text{ mm/day}$ ) is expected with more intensity ( $> 4 \text{ mm/day}$ ) in FF. Interestingly, the precipitation over northeast India and western India declines during the active periods in both NF and FF (Fig. 14c1–d1). It indicates that the heavy precipitation during the active days will be more localized or concentrated around the IGP and the northeastern parts of MCR. A similar analysis for the break composite illustrates the spatial pattern with a higher negative rainfall anomaly dominates over the entire MCR. Careful observation reveals that the precipitation not only declines at the MCR but also gradually decreases over most parts of the southern India and Himalayan foothills as well (Fig. 14a2–b2). The change in the precipitation anomaly of the break composite during FF reveals more decrease over the northern India, IGP and northern MCR ( $\sim 1\text{--}2 \text{ mm/day}$ ) compared to southern

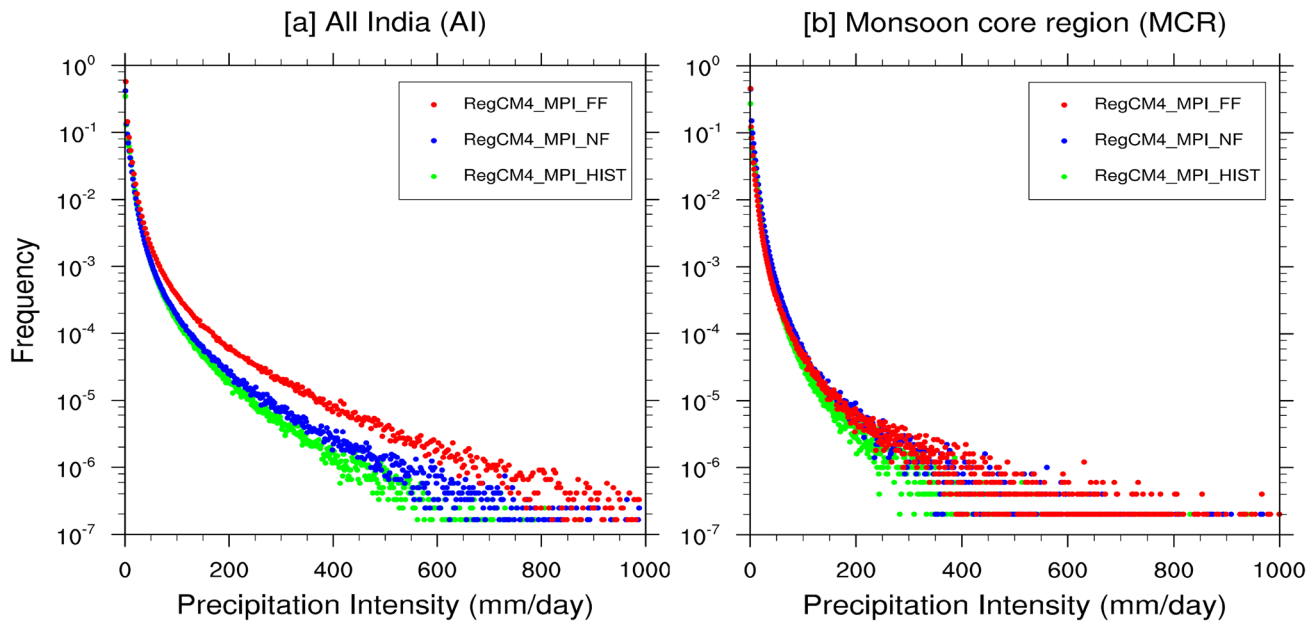


**Fig. 12** Probability density function (PDF) of daily mean precipitation over (a) All India, and (b) MCR during JJAS 1995–2014 (HIST), 2041–2060 (NF), 2080–2099 (FF) periods from the RegCM4\_MPI. Units are in  $\text{mm day}^{-1}$

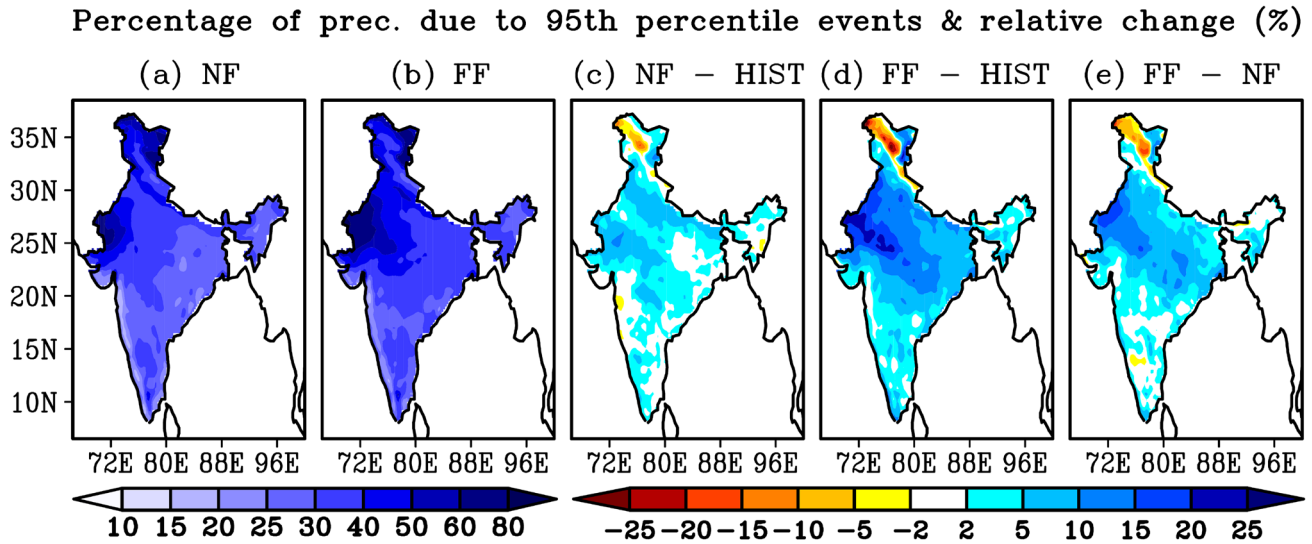


**Fig. 13** Percentage of precipitation (%) due to 95th percentile events during (a) NF, & (b) FF periods and the projected future relative changes (%) in the percentage of precipitation during (c) NF minus HIST, (d) FF minus HIST, and (e) FF minus NF from RegCM4\_MPI simulations

and western parts of India ( $\sim 0\text{--}1 \text{ mm/day}$ ) (Fig. 14c2). One interesting point that could be noted that the intensity of precipitation during the active period is higher relative to decreases in the precipitation during the break periods especially over the IGP in FF.

For the identification of possible causes, we additionally checked the changes in the SLP, NSLR and wind at 850 hPa during active and break phases in NF and FF (Fig. 15). RegCM shows a significant decline in the SLP by 150–200

over the MCR in both NF and FF periods. The spatial coverage of the decline of SLP is higher in NF as compared to FF i.e. the SLP values decline eastward towards the Bay of Bengal (BoB) (Fig. 15a1–a2). Correspondingly, the changes in the winds at 850 hPa during the active phases show consistent strengthen in FF compared to NF. In the FF, both the branches of winds i.e. moisture from the Arabian Sea and BoB strengthens which contributes to the increases in the precipitation in MCR (Fig. a5–a6). \*\*Further, the

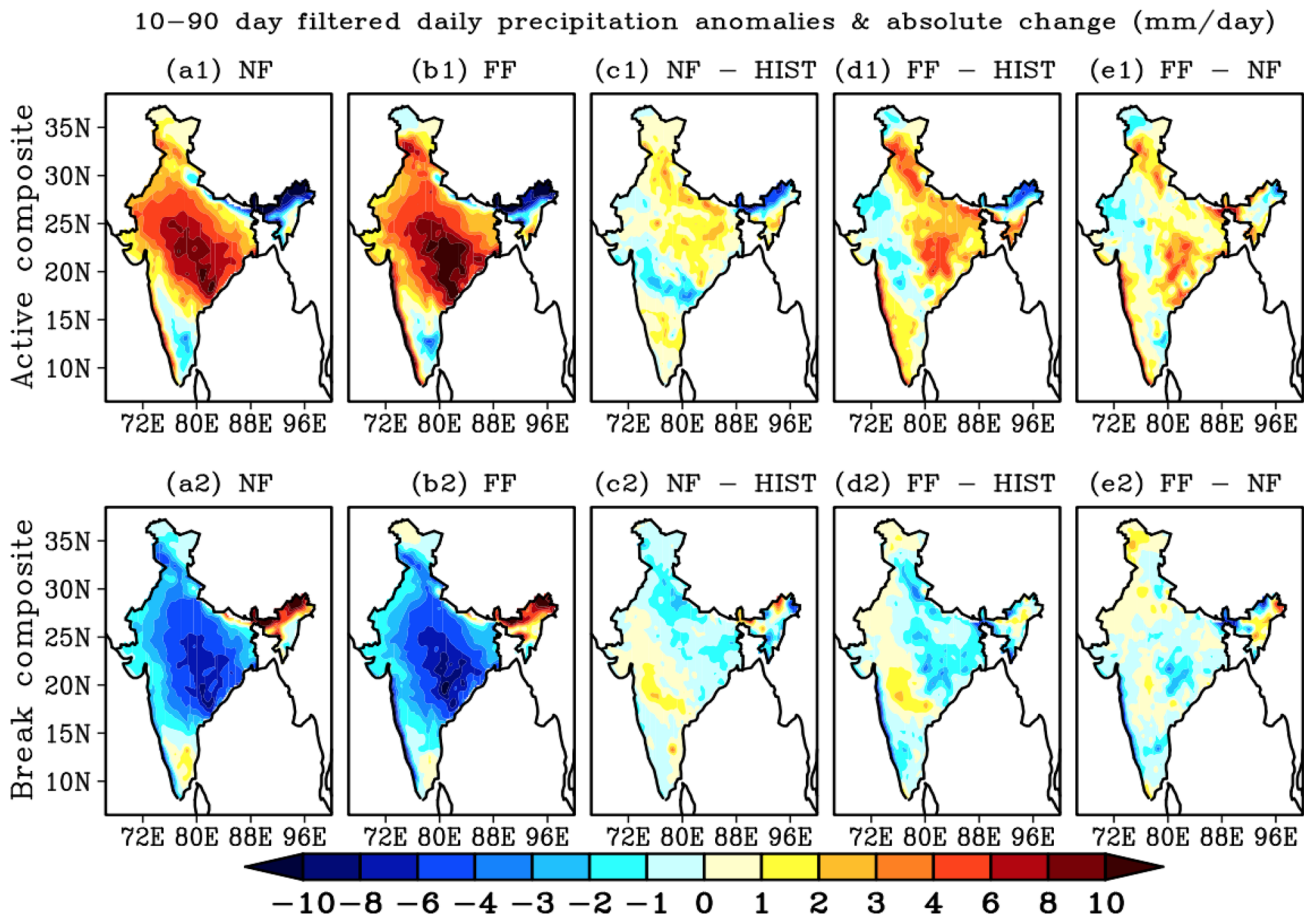


**Fig. 14** Active & break composites of 10–90 day filters daily precipitation anomalies ( $\text{mm day}^{-1}$ ) during (a1 & 2) NF, & (b1 & 2) FF periods and the projected absolute future changes in the precipitation

anomalies (c1 & 2) NF minus HIST, (d1 & 2) FF minus HIST, and (e1 & 2) FF minus NF as simulated by RegCM4\_MPI

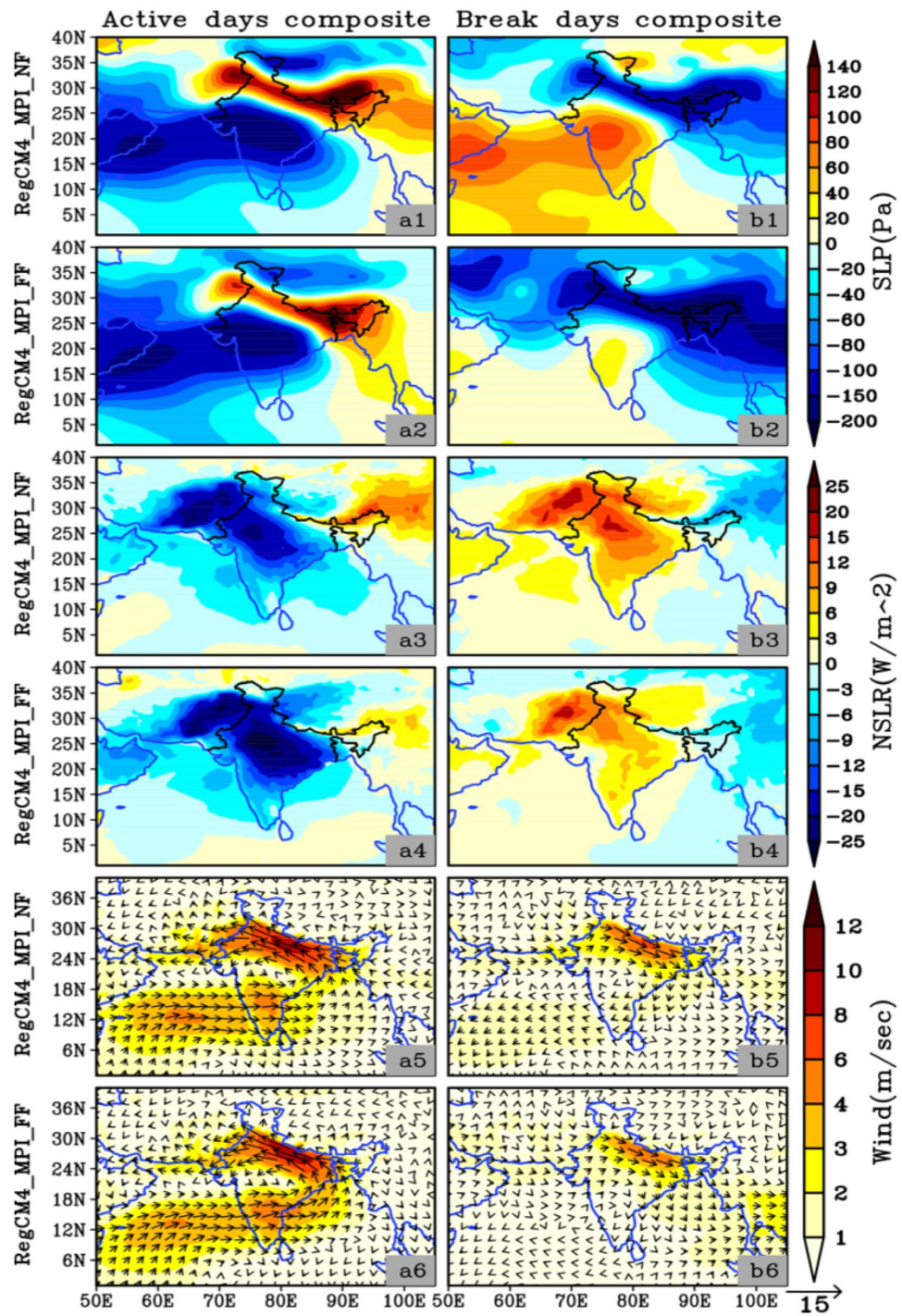
changes in the NSLR are also examined for NF and FF periods (Figs. 15a3–a4), which reflects the decrease in NSLR indicating an increase in the convective activities over the MCR regions. The signal is more dominant in FF with the flux values declined by more than  $25 \text{ Wm}^{-2}$ . On the other hand, the composite of the break spells shows the exact opposite signature as compared to the same from active spells (Fig. 14a2–b2). The increased SLP anomaly over MCR increases pressure over the landmass, which restricts the moisture-laden air to enter the landmass and resulted in the decline in the precipitation during the break phase of the ISM. Interestingly, unlike the increases in precipitation during active phases in moving from NF to FF ( $\sim 3\text{--}6 \text{ mm/day}$ ), there are relatively lesser decreases in precipitation during the break phases in FF ( $\sim 0\text{--}2 \text{ mm/day}$ ) over MCR. One of the reasons could be the lesser increase in SLP in FF compared to NF. As seen from Figs. 15b1–b2, the magnitudes of SLP anomalies are more over the Arabian Sea and western central India in NF, which gradually decreased in FF. This indicates that the break spells are likely to shrink

in FF, as there is increased precipitation during the break spells. Further, the increased anomaly of the NSLR suggests the decline in the formation of convective activities during the NF resulting in less precipitation, which weakens in FF leading to a favorable condition for the convection and hence precipitation (Figs. 15b3–b4). The anomalous northwesterly is strong during NF as compared to FF (Figs. 15b5–b6). The stronger the northwesterly the weaker is the moisture supply towards the mainland and MCR. This resulted in the decline in the precipitation in NF as compared to the FF.

#### 4 Summary and conclusions

In this work, we examine the recently compiled RegCM4 CORDEX-CORE simulations in replicating the characteristics of ISM. In particular, EIN75 and MPI-ESM-MR driven RegCM4 have been used to study the present and future projections of monsoon climate, its variability, and the associated dynamics under the RCP8.5 scenario. We

**Fig. 15** Active & break composites of (a1, b1, a2, b2) mean sea level pressure, (a3, b3, a4, b4) net surface longwave radiation and (a5, b5, a6, b6) wind anomalies for RegCM4\_MPI\_NF and RegCM4\_MPI\_FF; respectively



investigate the capability of RegCM4 in terms of capturing the spatial and temporal distribution of precipitation, wind circulations, mean and extreme precipitation, and intra-seasonality within the ISM i.e. active and break phases. Other variables like winds, SLP, NSLR are used to understand the variability in active and break spells in the present and future periods.

The main conclusions of the study are as follows:

1. The RegCM4 using both the boundary conditions i.e. EIN75 and MPI-ESM\_MPI are able to capture the spatial and temporal characteristics of ISM. Typical features include the development, mature and demise of the ISM precipitation with its northward propagation (latitude-time cross-section) is well-replicated in both cases in the prevailing conditions. RegCM4 simulated high precipitation regions such as the Western Ghats, northeast

- states well with close estimates over the monsoon core region with spatial accuracy. Future projections show substantial decreases in ISM precipitation of about 10–30% in the NF and 20–50% in the FF with maximum impact over northwest India. Additionally, changes in the mean annual cycle show increases in precipitation during later months of monsoon to post-monsoon (October–November) indicating a possible shift of precipitation regime in the FF.
2. The monsoon low-level winds with their maxima (> 18 m/s) over the Arabian Sea and direction towards the Indian sub-continent are also well represented by the simulations. The winds are, however, slightly weaker over the Indian landmass in the RegCM4\_MPI experiment. In future periods, the winds are expected to weaken over the Arabian sea and a northward shift of the winds is noted. This restricts the moisture influx from the Arabian Sea leading to a decrease in the ISM precipitation.
  3. In terms of extremes, the model performs better over the MCR regions coinciding with IMD observation, however; there is an overestimation of heavy to very heavy precipitation while considering all Indian sub-continent. Despite of limited observational rain gauges over the high mountainous regions, the overestimation of extremes could be partly attributed to the enhanced topographical forcing. From the PDFs, in the FF, the frequency as well as the magnitude of precipitation extremes is expected to increase over the Indian sub-continent. The most sensitive regions to precipitation extremes could be the northwest and parts of MCR regions.
  4. The spatial distribution of active and break precipitation composites is well represented in the RegCM4 with slightly stretched northwards. In particular, the model simulates accurately both active and break precipitation composites over the MCR region as compared to the observations. Our analysis shows an increase in the intensity of the precipitation during active spells in the NF and with a further increase in the intensity in FF. This is mostly due to the decrease in the SLP that initiates the winds to bring moisture from the Arabian Sea with an increase in the convective activities indicated by NSLR. On the other hand, during the break spell, the intensity of precipitation is expected to decrease in the future. Likewise, the decreases in precipitation in break spells are mostly due to an increase in the SLP and a decrease in the convective activities and over the Indian landmass.

In this paper, we mostly showcase the model's fidelity in determining the features of ISM and what might be future changes and associated dynamics employing an

MPI–ESM–MR driven RegCM4 model. Also, we present analysis using a regional climate model (RegCM4) in projecting changes of the intra-seasonal characteristics such as active and break spatial composites and the contribution from the dynamics that has not been well documented in the literature. However, for a more robust study, it is necessary to include more RCM ensemble members, which the authors would carry out in the future.

**Acknowledgements** The authors are thankful to the WCRP initiated CORDEX project which provided the data used in this study. All the variables analyzed are archived in the ESGF website <https://esgf-data.dkrz.de/search/cordex-dkrz/>.

**Funding** Not applicable.

**Data availability** The datasets used in this work are freely available at WCRP CORDEX: <https://esgf-data.dkrz.de/search/cordex-dkrz/>

**Code availability** The analysis code is available on request from the corresponding author.

## Declarations

**Conflicts of interest** The authors declare that they have no conflict of interest.

## References

- Ali H, Modi P, Mishra V (2019) Increased flood risk in Indian sub-continent under the warming climate. *Weather Clim Extrem* 25:100212. <https://doi.org/10.1016/J.WACE.2019.100212>
- Allen MR, Dube OP, Solecki W et al 2018: Framing and context. In: Global warming of 1.5 °C. An IPCC special report on the impacts of global warming of 1.5 °C above pre-industrial levels and related global greenhouse gas emission pathways, in the context of strengthening the global response to the threat of climate change, sustainable development, and efforts to eradicate poverty [Masson-Delmotte, V., P. Zhai, H.-O. Pörtner, D. Roberts, J. Skea, P.R. Shukla, A. Pirani, W. Moufouma-Okia, C. Péan, R. Pidcock, S. Connors, J.B.R. Matthews, Y. Chen, X. Zhou, M.I. Gomis, E. Lonnoy, T. Maycock, M. Tignor, and T. Waterfield (eds.)]. In Press.
- Ashfaq M, Cavazos T, Reboita MS et al (2020) Robust late twenty-first century shift in the regional monsoons in RegCM–CORDEX simulations. *ClimDyn*. <https://doi.org/10.1007/s00382-020-05306-2>
- Bader DC, Covey C, Gutowski Jr. WJ, Held IM, Kunkel KE, Miller RL, Tokmakian RT, Zhang MH (2008) Climate models: an assessment of strengths and limitations. U.S. Climate change science program synthesis and assessment product 3.1. Dept. of Energy, Office of Biological and Environ. Research, p124
- Bhaskaran B, Murphy JM, Jones RG (1998) Intraseasonal oscillation in the Indian summer monsoon simulated by global and nested regional climate models. *Mon Wea Rev* 126:3124–3134
- Bhatla R, Ghosh S (2015) Study of break phase of Indian summer monsoon using different parameterization schemes of RegCM4. *3. Int J Earth AtmosSci* 2:109–115
- Bhatla R, Ghosh S, Mandal B et al (2016) Simulation of Indian summer monsoon onset with different parameterization convection schemes of RegCM-4.3. *Atmos Res* 176:10–18

- Bhatla R, Ghosh S, Mall RK et al (2018) Regional Climate Model Performance in Simulating Intra-seasonal and Interannual Variability of Indian Summer Monsoon. *Pure Appl Geophys* 175:3697–3718
- Bollasina MA, Ming Y, Ramaswamy V (2011) Anthropogenic aerosols and the weakening of the South Asian summer monsoon. *Science* 334:502–505
- IPCC, 2007: Climate Change 2007: The Physical Science Basis. Contribution of Working Group I to the Fourth Assessment Report of the Intergovernmental Panel on Climate Change [Solomon, S., D. Qin, M. Manning, Z. Chen, M. Marquis, K.B. Averyt, M. Tignor and H.L. Miller (eds.)]. Cambridge University Press, Cambridge, United Kingdom and New York, NY, USA, 996 pp
- Chen X, Pauluis OM, Zhang F (2018) Regional simulation of Indian summer monsoon intraseasonal oscillations at gray-zone resolution. *Atmospheric ChemPhys* 18:1003–1022
- Choudhary A, Dimri AP, Maharana P (2018) Assessment of CORDEX-SA experiments in representing precipitation climatology of summer monsoon over India. *Theor Appl Climatol* 134(1):283–307
- Ciarlo JM, Coppola E, Fantini A et al (2020) A new spatially distributed added value index for regional climate models: the EURO-CORDEX and the CORDEX-CORE highest resolution ensembles. *Clim Dyn* 1–22. <https://doi.org/10.1007/s00382-020-05400-5>
- Das S, Dey S, Dash SK et al (2015) Dust aerosol feedback on the Indian summer monsoon: Sensitivity to absorption property. *J Geophys Res Atmos* 120:9642–9652
- Das S, Giorgi F, Giuliani G (2020b) Investigating the relative responses of regional monsoon dynamics to snow darkening and direct radiative effects of dust and carbonaceous aerosols over the Indian subcontinent. *Clim Dyn* 55. <https://doi.org/10.1007/s00382-020-05307-1>
- Das S, Giorgi F, Giuliani G et al (2020a) Near-future anthropogenic aerosol emission scenarios and their direct radiative effects on the present-day characteristics of the Indian summer monsoon. *J Geophys Res Atmos* 125. <https://doi.org/10.1029/2019JD031414>
- Dash S, Shekhar M, Singh G (2006) Simulation of Indian summer monsoon circulation and rainfall using RegCM3. *Theor Appl Climatol* 86:161–172
- Dash SK, Kulkarni MA, Mohanty UC, Prasad K (2009) Changes in the characteristics of rain events in India. *J Geophys Res Atmos* 114. <https://doi.org/10.1029/2008JD010572>
- Dash SK, Mishra SK, Pattnayak KC, Mamgain A, Mariotti L, Coppola E, Giorgi F, Giuliani G (2015) Projected seasonal mean summer monsoon over India and adjoining regions for the twenty-first century. *Theor Appl Climatol* 122(3):581–593
- Duchon CE (1979) Lanczos filtering in one and two dimensions. *J Appl Meteor* 18(8):1016–1022
- Emanuel KA, Živković-Rothman M (1999) Development and evaluation of a convection scheme for use in climate models. *J Atmos Sci* 56:1766–1782
- Feser F, Rockel B, von Storch H et al (2011) Regional climate models add value to global model data: a review and selected examples. *Bull Am Meteorol Soc* 92:1181–1192
- Ghosh S, Bhatla R, Mall RK et al (2019) Aspect of ECMWF down-scaled regional climate modeling in simulating Indian summer monsoon rainfall and dependencies on lateral boundary conditions. *Theor Appl Climatol* 135:1559–1581
- Giorgi F (2019) Thirty years of regional climate modeling: Where are we and where are we going next? *J Geophys Res Atmos* 124:5696–5723
- Giorgi F, Bates GT (1989) The climatological skill of a regional model over complex terrain. *Mon Weather Rev* 117:2325–2347
- Giorgi F, Gutowski W (2015) Regional dynamical downscaling and the CORDEX Initiative. *Annu Rev Environ Resour* 40:467–490
- Giorgi F, Jones, C, Asrar, GR (2009) Addressing climate information needs at the regional level: the CORDEX framework. *World Meteorological Organization (WMO) Bulletin* 58(3):175–183.
- Giorgi F, Coppola E, Solmon F et al (2012) RegCM4: model description and preliminary tests over multiple CORDEX domains. *Clim Res* 52:7–29
- Goswami BN (2012) South Asian monsoon. In: Lau WKM, Waliser DE (eds) *Intraseasonal variability in the atmosphere-ocean climate systems*, 2nd edn. Springer, Berlin, pp 21–72
- Goswami BN, Xavier PK (2005) Dynamics of “internal” interannual variability of the Indian summer monsoon in a GCM. *J Geophys Res* 110:D24104. <https://doi.org/10.1029/2005JD006042>
- Goswami BN, Wu G, Yasunari T (2006) The annual cycle, intraseasonal oscillations, and roadblock to seasonal predictability of the Asian Summer Monsoon. *J Clim* 19:5078–5099
- Grenier H, Bretherton CS (2001) A moist PBL parameterization for large-scale models and its application to subtropical cloud-topped marine boundary layers. *Mon Weather Rev* 129:357–377
- Halder S, Dirmeyer PA, Saha SK (2015) Sensitivity of the mean and variability of Indian summer monsoon to land surface schemes in RegCM4: Understanding coupled land atmosphere feedbacks. *J Geophys Res Atmos* 120:9437–9458
- Hersbach H, Bell B, Berrisford P et al (2020) The ERA5 global reanalysis. *Q J R Meteorol Soc* 146:1999–2049
- Kang IS, Yang YM, Tao WK (2015) GCMs with implicit and explicit representation of cloud microphysics for simulation of extreme precipitation frequency. *ClimDyn* 45:325–335
- Kiehl JT, Hack JJ, Bonan GB et al (1996) Description of the NCAR Community Climate Model (CCM3) (No. NCAR/TN-420+STR). University Corporation for Atmospheric Research. <https://doi.org/10.5065/D6FF3Q99>
- Maharana P, Dimri AP (2014) Study of seasonal climatology and inter-annual variability over India and its subregions using a regional climate model (RegCM3). *J Earth Syst Sci* 123:1147–1169
- Maharana P, Dimri AP (2016) Study of intraseasonal variability of Indian summer monsoon using a regional climate model. *ClimDyn* 46:1043–1064
- Maharana P, Dimri AP, Choudhary A (2019a) Redistribution of Indian summer monsoon by dust aerosol forcing. *Atmos Sci Lett* 26:584–596
- Maharana P, Kumar D, Dimri AP (2019b) Assessment of coupled regional climate model (RegCM4. 6-CLM4. 5) for Indian summer monsoon. *ClimDyn* 53:6543–6558
- Maharana P, Dimri AP, Choudhary A (2020a) Future changes in Indian summer monsoon characteristics under 1.5 and 2 °C specific warming levels. *ClimDyn* 54:507–523
- Maharana P, Kumar D, Das S, Tiwari PR (2020b) Present and future changes in precipitation characteristics during Indian summer monsoon in CORDEX-CORE simulations. *Int J Climatol*. <https://doi.org/10.1002/joc.6951>
- Mandke S, Sahai AK, Shinde MA, Joseph S, Chattopadhyay R (2007) Simulated changes in active/break spells during the Indian summer monsoon due to enhanced CO<sub>2</sub> concentrations: assessment from selected coupled atmosphere-ocean global climate models. *Int J Climatol* 27:837–859
- Maurya RKS, Mohanty MR, Sinha P, Mohanty UC (2020) Performance of hydrostatic and non-hydrostatic dynamical cores in RegCM4.6 for Indian summer monsoon simulation. *Meteorol Appl* 27. <https://doi.org/10.1002/met.1915>
- Medhaug I, Stolpe MB, Fischer EM, Knutti R (2017) Reconciling controversies about the ‘global warming hiatus.’ *Nature* 545:41–47
- Mukherjee S, Aadhar S, Stone D, Mishra V (2018) Increase in extreme precipitation events under anthropogenic warming in India. *Weather Clim Extremes* 20:45–53
- Oleson K, Lawrence DM, Bonan GB et al (2013) Technical description of version 4.5 of the Community Land Model (CLM) (No. NCAR/TN-503+STR). <https://doi.org/10.5065/D6RR1W7M>
- Pachauri RK, Allen MR, Barros VR et al (2014) Climate Change 2014: Synthesis report. Contribution of working groups I, II and III to

- the fifth assessment report of the intergovernmental panel on climate change / R. Pachauri and L. Meyer (editors), Geneva, Switzerland, IPCC, 151 p, ISBN: 978–92–9169–143–2
- Pai DS, Sridhar L, Rajeevan M et al (2014) Development of a new high spatial resolution ( $0.25^\circ \times 0.25^\circ$ ) long period (1901–2010) daily gridded rainfall data set over India and its comparison with existing data sets over the region. *Mausam* 65:1–18
- Pal JS, Small EE, Eltahir EA (2000) Simulation of regional-scale water and energy budgets: Representation of subgrid cloud and precipitation processes within RegCM. *J Geophys Res Atmos* 105:29579–29594
- Pattnayak KC, Panda SK, Saraswat V, Dash SK (2015) Relationship between tropospheric temperature and Indian summer monsoon rainfall as simulated by RegCM3. *ClimDyn* 46:3149–3162
- Paul S, Ghosh S, Oglesby R et al (2016) Weakening of Indian summer monsoon rainfall due to changes in land use land cover. *Sci Rep* 6:1–10. <https://doi.org/10.1038/srep32177>
- Rajeevan M, Gadgil S, Bhate J (2010) Active and break spells of the Indian summer monsoon. *J Earth Syst Sci* 119:229–247
- Rana A, Nikulin G, Kjellström E, Strandberg G, Kupiainen M, Hansson U, Kolax M (2020) Contrasting regional and global climate simulations over South Asia. *ClimDyn* 54(5):2883–2901
- Rogelj J, Forster PM, Kriegler E, Smith CJ, Séférian R (2019) Estimating and tracking the remaining carbon budget for stringent climate targets. *Nature* 571:335–342
- Roxy MK, Ghosh S, Pathak A et al (2017) A threefold rise in widespread extreme rain events over central India. *Nat Commun* 8:708. <https://doi.org/10.1038/s41467-017-00744-9>
- Rupa Kumar K, Sahai AK, Kumar KK, Patwardhan SK, Mishra PK, Revadekar JV, Kamala K, Pant GB (2006) High-resolution climate changes scenarios for India for the 21st century. *CurrSci* 90:334–345
- Sandeep A, Rao TN, Ramkiran CN et al (2014) Differences in atmospheric boundary-layer characteristics between wet and dry episodes of the Indian summer monsoon. *Bound-Layer Meteorol* 153:217–236
- Shahi NK, Rai S, Pandey DK (2016) Prediction of daily modes of South Asian monsoon variability and its association with Indian and Pacific Ocean SST in the NCEP CFS V2. *Meteorol Atmospheric Phys* 128:131–142
- Shahi NK, Rai S, Mishra N (2018a) Southern Indian Ocean SST as a modulator for the progression of Indian summer monsoon. *Theor Appl Climatol* 131:705–717
- Shahi NK, Rai S, Sahai AK, Abhilash S (2018b) Intra-seasonal variability of the South Asian monsoon and its relationship with the Indo-Pacific sea-surface temperature in the NCEP CFSv2. *Int J Climatol* 38:e28–e47
- Shahi NK, Rai S, Mishra N (2019) Recent predictors of Indian summer monsoon based on Indian and Pacific Ocean SST. *Meteorol Atmospheric Phys* 131:525–539
- Sharmila S, Joseph S, Sahai AK, Abhilash S, Chattopadhyay R (2015) Future projection of Indian summer monsoon variability under climate change scenario: an assessment from CMIP5 climate models. *Glob Planet Change* 124:62–78
- Singh S, Ghosh S, Sahana AS, Vittal H, Karmakar S (2017) Do dynamic regional models add value to the global model projections of Indian monsoon? *ClimDyn* 48(3):1375–1397
- Stone P, Risbey JS (1990) On the limitations of general circulation climate models. *Geophys Res Lett* 17:2173–2176
- Taraphdar S, Mukhopadhyay P, Goswami BN (2010) Predictability of Indian summer monsoon weather during active and break phases using a high resolution regional model. *Geophys Res Lett* 37:1–6
- Tollefson J (2020) How hot will Earth get by 2100? *Nature* 580:443–445
- Torma C, Giorgi F, Coppola E (2015) Added value of regional climate modeling over areas characterized by complex terrain-Precipitation over the Alps. *J Geophys Res Atmos* 120:3957–3972
- Torres-Alavez JA, Das S, Corrales-Suastegui A et al (2021) Future projections in the climatology of global low-level jets from CORDEX-CORE simulations. *ClimDyn*. <https://doi.org/10.1007/s00382-021-05671-6>
- Umakanth U, Kesarkar AP, Raju A, Rao SVB (2016) Representation of monsoon intraseasonal oscillations in regional climate model: sensitivity to convective physics. *ClimDyn* 47:895–917
- Victor DG, Kennel CF (2014) Climate policy: Ditch the 20C warming goal. *Nature* 514:30–31
- Waliser DE (2006) Interseasonal variability. In: Wang B (ed) *The Asian monsoon*. Springer, Berlin, pp 203–257
- Wang B (2012) Theories. In: Lau WKM, Waliser DE (eds) *Intraseasonal variability in the atmosphere-ocean climate system*, 2nd edn. Springer, Berlin, pp 335–398
- Xu Y, Ramanathan V, Victor DG (2018) Global warming will happen faster than we think. *Nature* 564:30–32

**Publisher's Note** Springer Nature remains neutral with regard to jurisdictional claims in published maps and institutional affiliations.